Wake downstream of the Lillgrund wind farm - A Comparison between LES using the actuator disc method and a Wind farm Parametrization in WRF

2015 J. Phys.: Conf. Ser. 625 012028

(http://iopscience.iop.org/1742-6596/625/1/012028)

Wake downstream of the Lillgrund wind farm - A Comparison between LES using the actuator disc method and a Wind farm Parametrization in WRF

O Eriksson[1], J Lindvall[2], S-P Breton[1], S Ivanell[1]

[1]Uppsala University, Department of Earth Sciences, Wind Energy Campus Gotland, 621 67 Visby, Sweden
[2]Kjeller Vindteknikk, Luntmakargatan 22, 111 37 Stockholm, Sweden

E-mail: ola.eriksson@geo.uu.se

Abstract.

Simulations of the Lillgrund wind farm (located between Malmö and Copenhagen) are performed using both Large Eddy Simulation (LES) and mesoscale simulations in WRF. The aim is to obtain a better understanding of wakes generated by entire wind farms in order to improve the understanding of farm to farm interactions. The study compares the results from the two used models for the energy production and the wake characteristics downstream of the wind farm. A comparison is also performed with regards to the production data from the Lillgrund wind farm which has been filtered to be comparable to the case used in the simulations.The studied case, based on a prerun in WRF without any wind farm, has an inflow angle of 222 $\pm$2.5 deg, a wind speed at hub height of 9.8 m/s and a near neutral atmosphere. A logarithmic wind shear is used in LES and the turbulence intensity is 5.9%.

The WRF simulations use a parameterization for wind farms. The wind farm is treated by the model as a sink of the resolved atmospheric momentum. The total energy extraction and the electrical power are respectively proportional to specified thrust and power coefficients. The generated turbulent kinetic energy are the difference between the total and the electrical power.

The LES are performed using the EllipSys3D code applying the actuator disc methodology for representing the presence of the rotors. Synthetic atmospheric turbulence is generated with the Mann model. Both the atmospheric turbulence and the wind shear are introduced using body forces.

The production was found to be better estimated in LES. WRF show a slightly higher recovery behind the farm. The internal boundary layer is for the compared simulation setups higher in LES while the wake expansion is about the same in both models. The results from the WRF parameterization could potentially be improved by increasing the grid resolution. For farm to farm interaction a combination of the two methods is found to be of interest.

1. Introduction

More and larger wind farms are planned offshore in Europe. One of the main reasons for this development is the good wind conditions offshore. The number of highly suitable sites for offshore wind farms is however limited by factors such as water depth and distance from shore. As more offshore wind farms are built there will be more occasions when the wake from one wind farm will interact with other close-standing wind farms. This expected development requires an increased understanding of the so-called farm to farm interaction in order to ensure a correct estimation of production and loads for future wind farms. It is therefore necessary to not only

study the near and far wakes behind single turbines and the interaction inside farms but also the long distance wakes impacting the wind conditions at neighboring sites.

It is known that wind farms produce long distance wakes [1]. The scale of the long distance wakes is in the order of 10 km [2]. Different types of wake and mesoscale models can be applied to simulate wind farm wakes [1][3]. Even Large Eddy Simulations (LES) are becoming feasible due to the increasing computational resources. LES have been used for the prediction of wakes inside wind farms in a wide range of studies [4][5][6][7][8][9][10][11]. LES with an actuator disc method was used to study the velocity recovery behind an infinitely wide wind farm [12].

Mesoscale models are used for atmospheric simulations and can by including parameterization of wind turbines [13] also be used to study the wakes behind farms.

LES and mesoscale models can be combined in two ways. The mesoscale output can be used as an input for the LES (1-way nesting) or the results obtained from this procedure can then even be fed back into the mesoscale simulation (2-way nesting) [14]. By combining the models one can take advantage of the relatively coarse grid in the mesoscale simulations which gives a good description of the atmosphere and the finer grid in LES which can resolve the wake flow.

In the current study the same case is studied both in the mesoscale model WRF (Weather Research and Forecasting Model) and in LES using an actuator disc method. This enables a comparison between the two models regarding the calculated energy production (also compared to wind farm data), the recovery of the flow behind the farm, the impact of the boundary layer and the expansion of the wake. The aim is to obtain a better understanding of wakes generated by entire wind farms in order to improve the understanding of farm to farm interactions.

2. Study of wakes in and behind the Lillgrund wind farm

The object of the simulations is the Swedish wind farm Lillgrund which is located between Malmö and Copenhagen. The wind farm consists of 48 Siemens wind turbines with a hub height of 65 m, a rotor radius (R) of 93 m and a rated power of 2.3 MW. A description of the Lillgrund wind farm is given by Nilsson [11] and in other earlier studies [15],[16]. Figure 1 displays the layout of the farm. The wake behind the farm is studied up to 7 km downstream.

One suitable atmospheric case with near neutral atmosphere and a relatively stable wind (regarding wind speed and direction) is found from presimulations without the wind farm in WRF. The studied wind direction is 222 deg +-2.5 deg where the wind is aligned with the rows. The wind shear determined from WRF along with the shear used in LES are shown in Figure 2. The turbulence intensity from WRF is 5.9% and the wind speed at hub height (U_0) is 9.82 m/s.

This case is then run in LES using an actuator disc method (see Section 2.1) and respectively in WRF with the wind farm parameterization (see Section 2.2). The production data from the site is filtered to be comparable to the simulated conditions (see Section 2.3). The comparison of the simulation results and measured production is presented in Section 3.

2.1. LES

Large Eddy Simulations (LES) resolve the largest most energetic eddies, while the smallest eddies are modeled using a subgrid-scale model. They can therefore be used to get a good description of the wake flow behind the wind turbines.

2.1.1. Numerical model The EllipSys3D code, non dimensionalized with R and U is used to carry out LES where the turbines are modeled according to an actuator disc method based on airfoil data [17]. The rotational speed of the turbines is individually controlled by a generator-torque algorithm in order to ensure a realistic and production optimized operation of every turbine throughout the simulation [18]. The subgrid-scale model from Ta-Phouc[19] is used for the small modeled eddies. The Mann model is used to pregenerate a realistic atmospheric

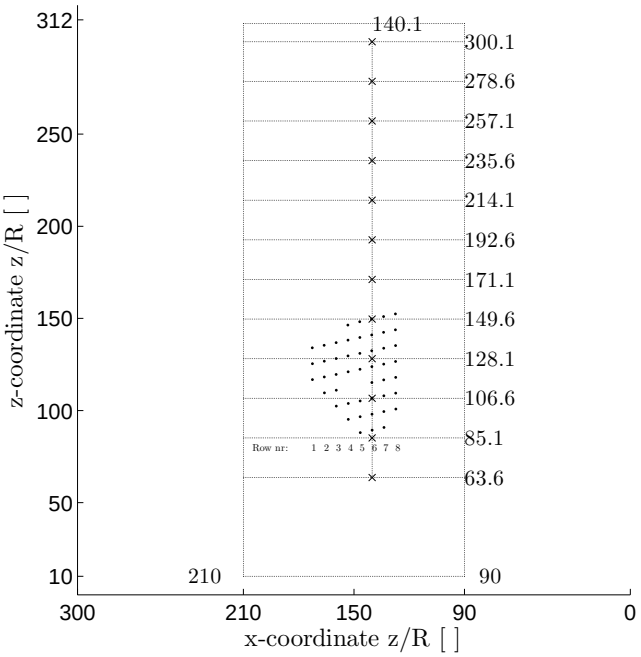

Figure 1. The placement of the turbines (•) in the domain covering 300 R * 322 R with the marked equidistant region of 120 R * 300 R. The flow is studied along the marked lines and for vertical profiles at the x's.

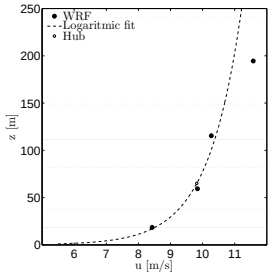

Figure 2. Logarithmic fit to the 3 lowest WRF-levels.

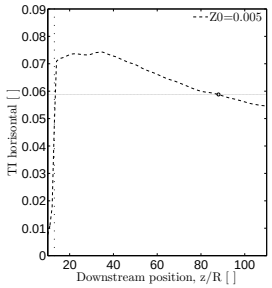

Figure 3. Downstream development of horizontal turbulence intensity (TI) at hub height (spanwise mean over 10 R).

turbulence [20][21]. The wind shear as well as the turbulence are imposed on the computational domain using body forces[10]. The model setup is considering a neutral boundary layer.

2.1.2. Simulation setup The simulations are performed for an area of 300 R in the spanwise/lateral direction (x) and 322 R in the streamwise/axial direction (z). This allows the wake to be studied to an extension of about 7 km behind the farm. In the region of interest the domain is equidistant. In Figure 1 the grid extensions, the equidistant area and the placement of the turbines can be seen. The farm is turned in such a way that a flow parallel to the z-axis corresponds to a wind direction of 222 degrees. The height (y-direction) of the equidistant region is 7.5 R (350m). The grid is stretched in the inlet (10 R), the outlet (10 R), towards the respectively side (90 R) and towards the top (up to the height of 50 R). This gives an equidistant region with 120 R width, 7.5 R height and 300 R length. The boundary conditions are fixed values for the inlet (according the wanted wind shear), cyclic for the sides, convective for the outlet, far field for the top and for the ground. The far field for the ground is setup to function as a noslip condition. The resolution (dx) in the equidistant region is 0.1 R (4.65 m) and in order to fulfill the CFL condition in a conservative way a non dimensionalized (with U_0 and R) timestep of 0.025 is used. The grid consists of 400 M cells.

The wind shear used is calculated using a logarithmic fit to the three lowest grid points in WRF, to get the most comparable shear at the turbine height, see Figure 2. The profile that has a wind speed of 9.82 m/s at hub height can be obtained from Equation 1.

$$U(z) = \frac{u_*}{\kappa} * ln\Big(\frac{z}{z_0}\Big) = 1.0366 * ln\Big(\frac{z}{0.005}\Big) \quad (1)$$

The Mann turbulence is created using the same roughness length (z_0) of 0.005 m and the wind speed 9.82 m/s at the hub height of 65 m as in the logarithmic wind shear used. In a simulation without turbines (in a similar but shorter and narrower grid) the downstream development of

the turbulence has been studied at hub height, see Figure 3. It can be seen that the turbulence intensity first increases and goes towards a value just below 6% further downstream. The first turbine is therefore placed on the domain at z=88 R where the horizontal turbulence intensity is 5.9% (the same level as in WRF). The turbulence planes are imposed to the domain at z=13 R and are convected downstream by the flow. The Mann box has an axial length of 10 min using the Taylor frozen hypothesis and it covers the equidistant region in x-y (120 R * 8 R) well with a resolution of 1.17 dx /1.25 dx/1.237 dx (width/height/length).

In two of the flow cases the flow is turned ±2.5 deg from 222 deg. The grid, the placement of the turbulence fields and the placement of the turbines remain unchanged. The inlet wind shear is however turned 2.5 deg and the turbines are yawed. To be normal respectively parallel to the incoming flow the fluctuations in the Mann box are therefore turned (but the Taylor frozen hypothesis is still used based on the assumption that the flow is aligned with the z-axis).

The airfoil data used in this study is based on the NREL 5 MW turbine [22] and scaled down to correspond to a Siemens SWT93-2.3MW turbine regarding both power and thrust coefficients [11] . The turbines are controlled by a generator-torque algorithm which is applied up to the point where the rated power is reached [18]. A pitch controller would be needed in order to handle higher wind speeds. However, the impact on the results is limited since there are only a few occasions in which the first turbines of the rows experience wind speeds above the rated wind speed. In these cases the rotational speed of these turbines only show a minor increase over a short period before it adjusts itself back to a value under the critical level.

The simulations first run for 20,000 timesteps, allowing the flow to establish and to pass through the entire domain length. The flow is thereafter studied for 40 min to get mean values of the flow variables. The result for the flow sector 222 deg ± 2.5 deg is finally calculated as the mean of the simulations for the three directions 219.5 deg, 222 deg and 224.5 deg.

2.2. Mesoscale simulations

The Weather Research and Forecasting (WRF) Model is a mesoscale model used in atmospheric research and numerical weather predictions. The model was created and is maintained by the National Center for Atmospheric Research (NCAR). Version v3.5.0 is used in this study and a further description of the model can be found in the technical note [23].

2.2.1. Numerical model WRF provides a parameterization for wind farms that uses a turbine drag coefficient [13], [24]. This parameterization is here used to simulate the wind farm for the chosen case. The wind farm is treated by the model as a sink of the resolved atmospheric momentum. The total energy extraction is a function of the wind speed and proportional to a specified generic thrust coefficient. The electrical power is also a function of the wind speed but proportional to a specified generic power coefficient. The generated turbulent kinetic energy is the difference between the total energy extraction and the electrical power. The fraction of the resolved atmospheric momentum that is extracted is given by specified thrust coefficients.

2.2.2. Simulation setup The first simulation is performed without any wind turbines. A second simulation is performed with the same setup as the first one but with the wind farm implemented according to the parameterization described above [13], [24]. The model is run with data from ERA Interim reanalysis [25] as input on the boundaries. WRF uses a nested grid with a horizontal resolution of 333m * 333m in the region of interest. The lowest vertical grid points (18 m, 59 m, 116 m, 195 m and 295 m) are given in Figure 2.

The studied result is the difference between the case run with and without the wind farm parameterization. The chosen case is characterized by a wind direction in the interval of 222 ± 2.5 deg lasting for more than 10 min. The stability is near neutral on the stable side (the potential temperature gradient is 0.6 K/km from sea surface up to 115m).

2.3. Production data

The production data is based on SCADA data collected over 5 years [15]. The data is filtered to include the inflow angles from 219.5 to 224.5 degrees and the wind speed interval of 9.82 m/s +-0.5 m/s. The stability classes that are included are near unstable, neutral and near stable, based on the Monin Obukhov length in the range of $L <$ -500 or $L >$500.

3. Results

The following sections provide a comparison between WRF and LES regarding relative production, velocity recovery, boundary layer development and wake expansion. Figure 1 shows the turbines and the position of the data outtakes. The data has been interpolated from the LES and WRF results. The wake is visualized based on the LES results in Figures 20 and 21.

The presented turbulence intensity is defined as the root mean square of the fluctuations (in z for streamwise and x for horizontal) divided by U_0 giving the real turbulence intensity for a wind speed equal to U_0 and a relative measure of the turbulent energy in all other cases. The generated turbulent kinetic energy from the farm is called Excess TKE and is defined as the the difference between the TKE in the wake and before the farm. The velocity deficit is in a similar way defined as the velocity reduction compared to the undisturbed wind before the farm. The results are non dimensionalized with R and U_0.

3.1. Production

The relative production (normalized with the mean of the measured production for the front turbines of rows 5-7) is shown in Figures 4-11.

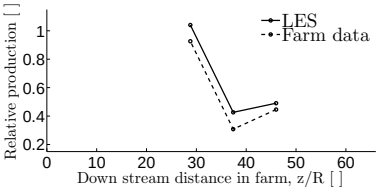

Figure 4. Row 1.

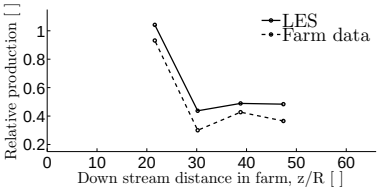

Figure 5. Row 2.

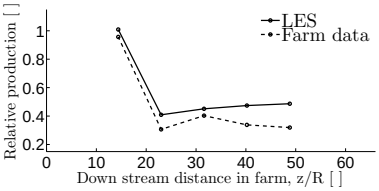

Figure 6. Row 3.

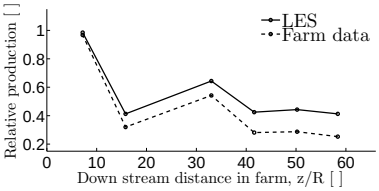

Figure 7. Row 4.

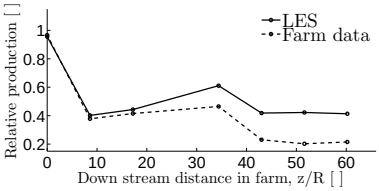

Figure 8. Row 5.

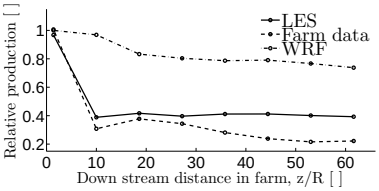

Figure 9. Row 6.

Figures 4-11 The relative production normalized with the mean of the production (SCADA-data) of the first turbines in rows 5-7. (In WRF normalized with the first turbine in the row.)

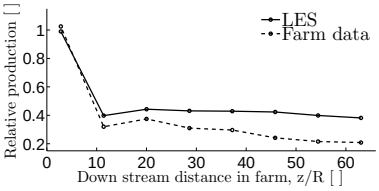

Figure 10. Row 7.

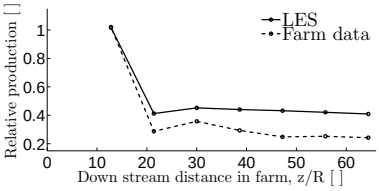

Figure 11. Row 8.

The distances are relative to the first turbine at z=88 R. The LES results follow the trend of the farm data relatively well. The production is however slightly overpredicted in the LES results, which is more pronounced towards the end of the farm. For rows 1-3 the front turbines also show higher values in the LES case. This can partly be explained by the fact that the farm data also includes partially stable atmospheric conditions which have lower turbulence intensity levels and a higher power deficit compared to the neutral conditions [15]. The averaging used over the sector in LES might also give too much weight to the $\pm$2.5 deg inflow. The LES results

also assume the same turbine efficiency (electrical/aero dynamic power) for all wind speeds, which might be lower in reality for partial loads. For row 6 the results from WRF can also be seen. The WRF parameterization used gives too high production. An explanation for this could be the low (333m) resolution of the grid.

3.2. Velocity recovery

Figures 12-15 show the downstream flow development at hub height along row 6 (the dotted lines indicate the turbine positions).

The LES results in Figure 12 show that inside the farm the downstream development of the wind speed (oscillating between 0.4 and 0.6) is relatively stable. Behind the farm the velocity in LES recovers to 0.81 at 2km, 0.86 at 4km and 0.907 at 6 km (for comparison the measured values behind the Horns Rev wind farm are around 0.85 at 2 km and 0.9 at 6 km [12]). The velocity deficit in Figure 13 shows clearly lower values inside the farm for WRF compared to LES. This (likewise the higher production in WRF) can be partially explained by the low grid resolution. The velocity reduction determined by the parametrization is here distributed over 1-2 cells of 333m in width and 3 cells/ 0-159 m in height. The downstream turbines experience consequently a slightly lower mean wind speed, but no full wake situation. WRF gives, as expected considering the behavior inside the farm, also higher velocities behind the wind farm (around 0.82 at 2 km and 0.95 at 6 km), but the differences are not as significant as in the farm.

The streamwise turbulence intensity in LES is 6.5% before the farm (at z=63.8 R), see Figure 14. Inside the farm the turbulence intensity increases for the 4 first turbines until a stable maximum value of around 14 % is reached. Behind the farm the turbulence intensity decreases over a few km down to a value of 7 %. The Excess TKE can be seen in Figure 15. It is clear that the value in WRF is much higher than LES's. This is also seen in other studies [26]. This could be explained by the fact that in WRF all the energy that is taken out from the flow either becomes electrical power or TKE, neglecting for example the efficiency of the turbine drive train [13]. Also the differences between the used C_T-curves could have an impact. The higher TKE level gives higher mixing and a faster velocity recovery.

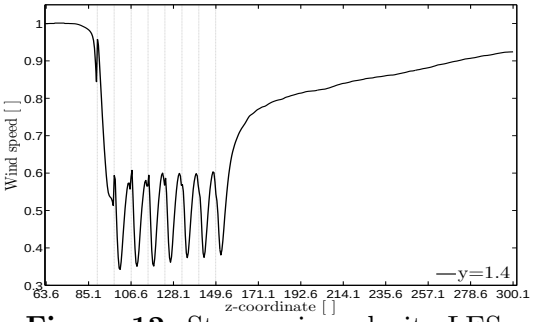

Figure 12. Streamwise velocity LES.

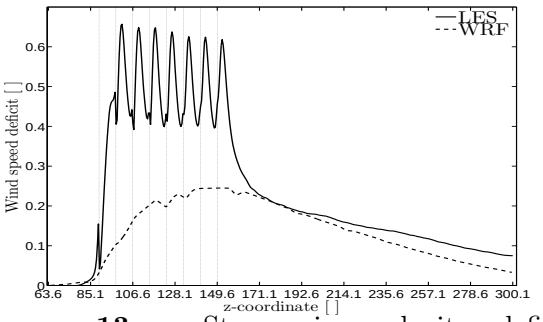

Figure 13. Streamwise velocity deficit (compared to z=63.8 R) , LES and WRF.

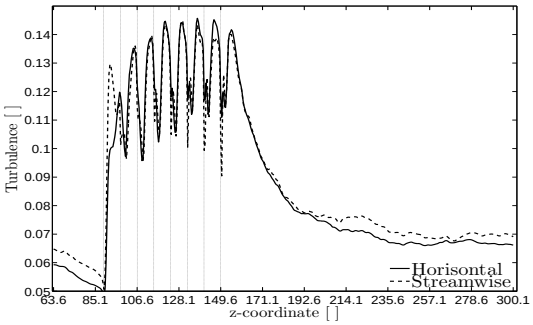

Figure 14. Horizontal and streamwise turbulence intensity LES.

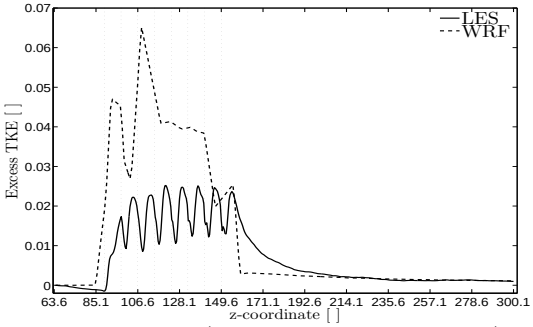

Figure 15. TKE (compared to z=63.8 R), LES and WRF.

3.3. Boundary layer

Figures 16-19 show the vertical profiles taken at each km along row 6 (before, in and behind the farm).

The two first wind shear profiles (from LES), representing the flow upstream of the farm, follow the logarithmic inlet wind shear relatively well, see Figure 16. The three next profiles are inside the farm and show the development of the internal boundary layer. The impact of the farm can be seen up to the height of around 4.2 R at 106.6 R , 5.7 R at 128.1R and 6.25 R over the last turbine at 149.6 R. Also after the farm an increased impact at greater heights can be seen. At the height of the rotor plane (0.4-2.4 R) the wind shear is almost vertical for the first profiles after the wind farm. The slope may increase slightly, but even after 7 km the shear is less sharp compared to the inlet. The turbulence intensity shows a similar vertical development resulting in increased turbulence intensity at greater heights downstream, see Figure 18.

A comparison between the wind shear profiles in LES and WRF is made in Figure 17. A lower velocity deficit at the height of the rotor plane can be noticed in WRF, especially in but also behind the farm. The LES method gives also a larger decrease in wind speed at greater heights. The resulting shear after the wind farm (estimated from the velocity deficit) is sharper in WRF compared to LES. The sharper shear in WRF compared to LES could (due to increased momentum transport) explain the faster velocity recovery in the farm wake. The TKE levels are higher in WRF, both inside the farm and at greater heights, Figure 19.

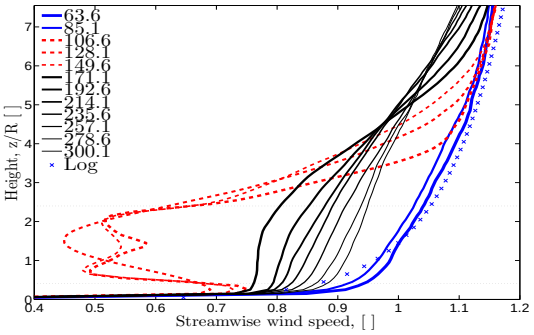

Figure 16. Streamwise velocity LES.

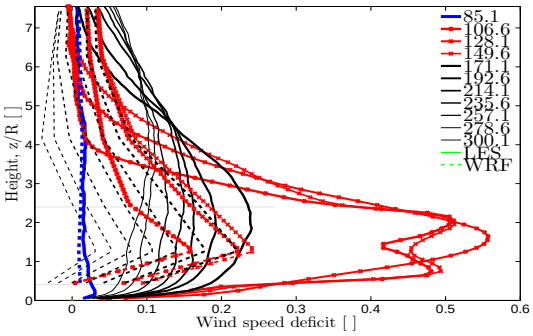

Figure 17. Streamwise velocity deficit (compared to z=63.8 R), LES and WRF.

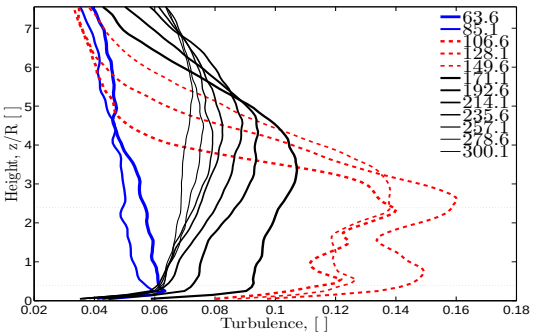

Figure 18. Horizontal turbulence intensity LES.

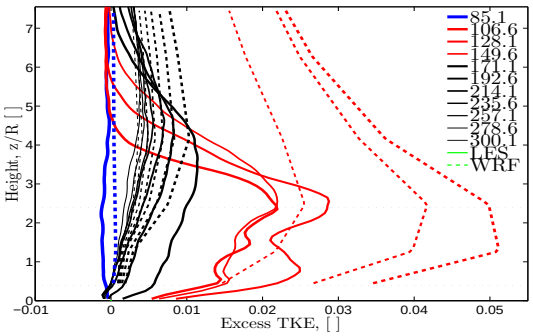

Figure 19. TKE (compared to z=63.8 R), LES and WRF.

3.4. Wake expansion

Figure 22 shows the wind speed along a spanwise line at hub height and Figure 24 the respective turbulence intensities in the LES case. The wind speed at the two first lines before the farm varies around 1. The following lines show the positions 1-7 km behind the farm. The values for the different lines follow the expected trend considering the number of turbines in each row (dotted lines) . The wake expansion downstream can be seen and outside the wake a slight

acceleration of the flow can be found. As expected, the expansion is slightly larger towards the right as the wake flow is more decelerated on that side due to the longer rows. The extensions of the wake can also clearly be seen in Figures 20 and 21 which covers the wake flow up to 150 R / 6 km behind the farm.

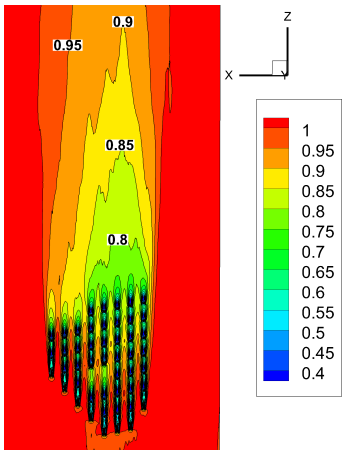

Figure 20. Streamwise velocity at hub-height from the equidistant region in LES.

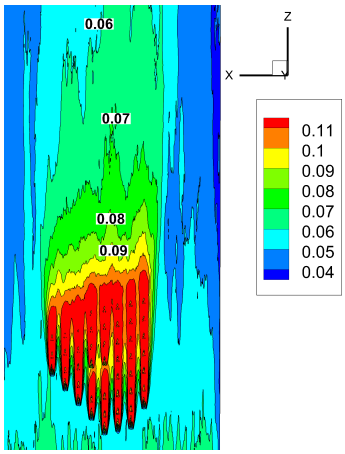

Figure 21. Horizontal turbulence intensity at hub height in LES.

The wake expansion is in the same order in WRF and LES, see Figure 23. In the WRF result an unexpected large acceleration can be seen for the left side. The excess TKE is also in the same order, except closest to the farm where the levels are higher in LES, see Figure 25. In LES the expansion of TKE is slightly larger. The general level of TKE outside the wake and downstream of the farm is lower in the LES.

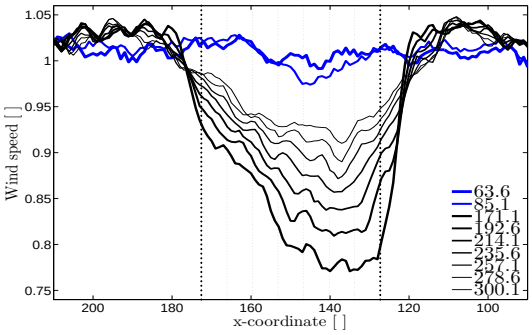

Figure 22. Streamwise velocity LES.

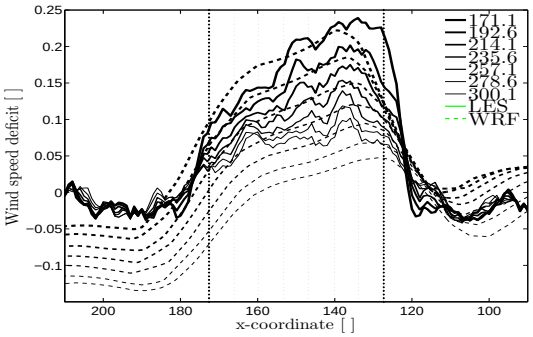

Figure 23. Streamwise velocity deficit (compared to z=63.8 R) , LES and WRF.

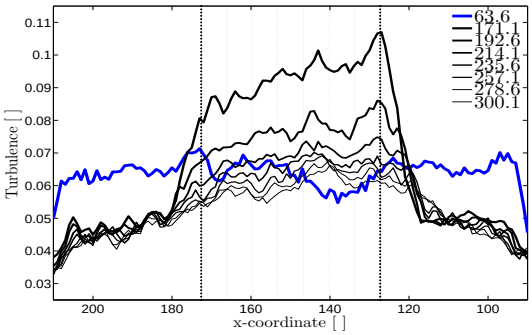

Figure 24. Horizontal turbulence intensity LES.

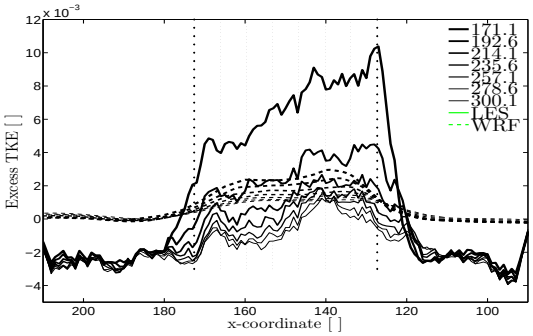

Figure 25. TKE (compared to z=63.8 R), LES and WRF.

4. Conclusion

One neutral flow case for the Lillgrund wind farm has been simulated both in the MESO-scale model WRF and as an LES with an actuator disc method. The input wind profile and turbulence intensity for the LES has been taken from WRF. The results have been compared with respect to the calculated energy production (also compared to wind farm data), the recovery of the flow behind the farm, the boundary layer development and the expansion of the wake.

The LES was shown to slightly overpredict production compared to the farm data, while WRF clearly overestimated the production.

The velocity reduction inside the farm is significantly larger for LES compared to WRF. For the recovery of the flow behind the farm a slightly faster recovery is seen in WRF.

Regarding the impact of the farm on the development of the boundary layer, a reduction of velocity could be found at greater heights in the LES as compared to WRF. For the turbulence intensity the increase was found to be larger in the WRF results. The estimated slopes of the shear profiles are higher in WRF indicating a larger downward momentum transport. The expansion of the wake was in the same order in both simulation models.

The main differences between the results could be related to the lower grid resolution in WRF and the higher TKE levels added from the parameterization. The low grid resolution in WRF causes a smearing of the velocity deceleration from the turbine parametrization over a large cross section. This results in an increased production for the downstream turbines. Although the outtake of energy from the flow by the turbines in WRF is larger, a lower wake deficit behind the wind farm was seen in this case. This could be due to the sharper resulting shear and the related downward momentum transport. It has to be pointed out that the comparison is performed for one specific flow occasion in WRF. The introduced uncertainties could have been reduced by averaging over a number of similar flow cases.

The production results from LES show relatively good agreement with production results from Lillgrund. For the farm wake flow no site data is available but comparing to measurements on Horns rev the velocity recovery is in the same order at 2 km and 6 km behind the farm.

The differences between the results indicate that the results from LES are in better agreement with the farm data. The needed computational resources are however much larger. WRF could potentially give better results with a higher resolution over the farm. The results from LES could possibly be used to adopt the WRF parameterization for the downstream turbine.

To get better understanding of farm to farm interaction a first step is to study the wake behind entire wind farms. Some differences in the results from WRF and LES were here pointed out. The production was especially shown to be closer to the farm production in the LES case. The velocity recovery was reasonable in LES. The WRF case showed a slightly faster velocity recovery. For farm to farm interaction studies it can be of interest to combine the two models to take advantage from both the relatively coarse grid in the mesoscale simulations which gives a good description of the atmosphere and the finer grid in LES which can resolve the wake flow. One alternative is to nest LES into the WRF simulations, this would however be more computational demanding. A potential configuration for future farm to farm interaction studies could be to use WRF for the first wind farm and then use the farm wake flow conditions as an input (similar to what was done in this study for the inlet profile) for a LES of the second wind farm.

Acknowledgments

The LES were performed on resources provided by the Swedish National Infrastructure for Computing (SNIC) at the National Supercomputer Centre in Sweden (NSC). The WRF-simulations were performed on the Abel Cluster, owned by the University of Oslo and the Norwegian meta center for High Performance Computing (NOTUR), and operated by the Department for Research Computing at USIT, the University of Oslo IT-department. http://www.hpc.uio.no/. Jan-Åke Dahlberg at Vattenfall AB is acknowledged for providing

measurement data from the Lillgrund wind farm as well as Kurt Hansen at DTU Wind for post processing of these data. This work was supported financially by the Top-Level Research Initiative (TFI) project, Improved Forecast of Wind, Waves and Icing (IceWind) and Vindforsk IV.

References

[1] Frandsen S, Barthelmie R, Rathmann O, Jørgensen H, Badger J, Hansen K, Ott S, Rethore P, Larsen S and Jensen L 2007 *Summary report: The shadow effect of large wind farms: measurements,data analysis and modelling.* (Risø-R-1615(EN), Denmark)

[2] Eriksson O and Ivanell S 2012 *A survey of available data and studies of farm-farm interaction.* (EAWE PhD Seminar on Wind Energy in Europe, 2012)

[3] Brand A 2009 *Wind Power Plant North Sea – Wind farm interaction, The effect of wind farming on mesoscale flow.* (ECN, the Neatherlands)

[4] Ivanell S 2009 *Numerical Computations of Wind Turbine Wakes.* (PhD thesis, ISBN 978-91-7415-216, KTH Engineering Sciences, Sweden)

[5] Lu H and Porté-Agel F 2011 *Large eddy simulation of a very large wind farm in a stable atmospheric boundary layer.* (Physics of Fluids 2011; 23: 065101)

[6] Wu Y T and Porté-Agel F 2012 *Atmospheric turbulence effects on wind-turbine wakes: An LES study.* (Energies 2012, 5, 5340-5362)

[7] Troldborg N, Sørensen J N and Mikkelsen R 2010 *Numerical simulations of wake characteristics of a wind turbine in uniform inflow.* (Wind Energy 2010; 13: 86–99)

[8] Troldborg N, Larsen G C, Hansen K S, Sørensen J N and Mikkelsen R 2011 *Numerical simulations of wake interaction between two wind turbines at various inflow conditions.* (Wind Energy 2011; 14: 859–876.)

[9] Keck R E, Mikkelsen R, Troldborg N, de Maré M and Hansen K S 2013 *Synthetic atmospheric turbulence and wind shear in large eddy simulations of wind turbine wakes.* (Wind Energy 2013; DOI: 10.1002/we.1631)

[10] Troldborg N, Sørensen J N, Mikkelsen R and Sørensen N N 2014 *A simple atmospheric boundary layer model applied to large eddy simulations of wind turbine wakes.* (Wind Energy 2014; 17: 657-669.))

[11] Nilsson K, Ivanell S, Hansen K S, Mikkelsen R, Breton S P and Henningson D 2014 *Large-eddy simulations of the Lillgrund wind farm.* (Wind Energy 2014; DOI: 10.1002/we.1707)

[12] Eriksson O, Mikkelsen R, Nilsson K and Ivanell S 2012 *Analysis of long distance wakes of Horns rev 1 using actuator disc approach.* (J. Phys.: Conf. Ser. 555 012032)

[13] Fitch A C, Olson J B, Lundquist J K, Dudhia J, Gupta A K, Michalakes J and Barstad I 2012 *Local and Mesoscale Impacts of Wind Farms as Parameterized in a Mesoscale NWP Model.* (Monthly Weather Review, Volume 140, Issue 9 .)

[14] Lundquist J K, Mirocha J D and Kosovic B 2010 *Nesting large-eddy simulations within mesoscale simulations in WRF for wind energy applications.* (Proceedings of the Fifth International Symposium on Computational Wind Engineering, Chapel Hill, NC)

[15] Hansen K S 2013 *Preliminary benchmark for Lillgrund performed in EERA-DTOC.* (EERA-DTOC. Presentation DTU 20th June 2013.)

[16] Churchfield M, Lee S, Moriarity P J, Martinez L A, Leonardi S, Vijayakumar G and Brasseur J G 2012 *A Large-Eddy Simulation of Wind-Plant Aerodynamics.* (NREL, the United states of America)

[17] Mikkelsen R 2003 *Actuator Disc Methods Applied to Wind Turbines.* (DTU, Denmark)

[18] Breton S P, Nilsson K, Ivanell S, Olivares-Espinosa H, Masson C and Dufresne L 2012 *Study of the effect of the presence of downstream turbines on upstream ones and use of a controller in CFD wind turbine simulation models.* (J. Phys.: Conf. Ser. 555 012014)

[19] TaPhouc L 1994 *Modéles de sous maille appliqués aux écoulmements instationnaires décollés.* (Tech. rep. LIMSI 93074 LIMSI France.)

[20] Mann J 1998 *Wind field simulation.* (Risø, Denmark)

[21] Jakob M, Ott S, Jørgensen B H and Frank H P 2013 *WAsP Engineering 2000.* (Risø–R–1356(EN))

[22] Jonkman J, Butterfield S, Musial W and Scott G 2009 *Wind Turbine for Offshore System Development.* (NREL, the United states of America)

[23] Skamarock W C, Klemp J B, Dudhia J, Gill D O, Barker D M, Duda M G, Huang X, W W and Powers J G 2008 *A Description of the Advanced Research WRF Version 3.* (Technical Note NCAR/TN-475+STR)

[24] Fitch A C, Olson J B, Lundquist J K, Dudhia J, Gupta A K, Michalakes J, Barstad I and Archer C L 2013 *Corrigendum.* (Monthly Weather Review, 141, 1395–1395.)

[25] Dee D P and et al 2011 *The ERA-Interim reanalysis: configuration and performance of the data assimilation system.* (Q.J.R. Meteorol. Soc., 137: 553–597)

[26] Abkar M and Porté-Agel F 2015 *A new wind-farm parameterization for large-scale atmospheric models.* (Journal of Renewable and Sustainable Energy, 7.1: 013121)